Analytical Approach for MRI RF Array Coils Decoupling by Using Counter-Coupled Passive Resonators

DANILO BRIZI [1,2] (Member, IEEE), **NUNZIA FONTANA** [2,3] (Member, IEEE),

AND AGOSTINO MONORCHIO [1,2] (Fellow, IEEE)

[1] Department of Information Engineering, University of Pisa, 56122 Pisa, Italy
[2] Consorzio Nazionale Interuniversitario per le Telecomunicazioni, Rass Lab, 56122 Pisa, Italy.
[3] Department of Ingegneria dell'Energia, dei Sistemi, del Territorio e delle Costruzioni, University of Pisa, 56122 Pisa, Italy

CORRESPONDING AUTHOR: D. BRIZI (e-mail: danilo.brizi@ing.unipi.it)

ABSTRACT We introduce an analytical approach to design decoupling filters for MRI radiofrequency array elements, adopting counter-coupled passive resonators as unit-cells. Specifically, our method is based on a magneto-static hypothesis, thus a deep comprehension of the physical interactions between all the elements in the system and design guidelines can be achieved. In particular, the couplings between adjacent and next-nearest neighbors coils pairs are both modeled, hence addressing the requirements for MRI arrays. The analytically-obtained filter solution is subsequently refined resorting to targeted full-wave simulations, reducing the computational effort. To prove the validity of the proposed approach, we conceived a test-case consisting of three planar RF coils, tuned at the 7T proton Larmor frequency. We demonstrated through full-wave simulations that the analytical design method is accurate and effective. Moreover, we fabricated a prototype and we performed benchtop measurements, both in unloaded conditions and in the presence of a biological phantom, resulting in excellent agreement with simulations. The developed analytical framework can be useful to model and control the mutual interactions between the various elements of an RF MRI system. In addition, the possibility to print the decoupling elements and the RF coils on the same dielectric substrate leads to a mechanically robust prototype.

INDEX TERMS Decoupling, distributed magnetic traps (DMTs), radiofrequency array, magnetic resonance imaging (MRI), mutual decoupling, radio frequency (RF) coil, spiral resonators (SRs).

I. INTRODUCTION

MUTUAL coupling between RF coils is a most important concern in Magnetic Resonance Imaging (MRI). Indeed, the MRI research activities are progressively pushing the applied static magnetic field amplitude towards higher and higher values in order to increase, as it is well known, the Signal-to-Noise Ratio (SNR) and the imaging spatial resolution [1]–[3]. However, this technical choice leads to a natural consequence, i.e., higher operative frequencies for the RF coils, as dictated by the Larmor's relationship. In this condition, realizing a single large RF coil able to cover the desired field of view (FoV) becomes hardly practicable [4], [5]. As a matter of fact, the electromagnetic wavelength is rapidly approaching the coil dimension and,

thus, the homogeneity of the RF magnetic field is spoiled, and electric field hot spots can arise. In order to reduce this problem, parallel imaging has been introduced [6]; instead of employing a single large RF coil, a transceiver array of RF coils in which every element is fed with the appropriate amplitude and phase (phased array concept) can be adopted to generate a homogeneous magnetic field. This solution can also reduce undesired hot spots in the tissues (lower Specific Absorption Rate, SAR), even at relatively high operative frequencies. In addition, the FoV can be increased as well as the sensitivity during the receiving phase (better SNR). Moreover, the scan time can be significantly reduced, thus improving the overall performance of the MRI scanners [7]–[14].

Nonetheless, such array configurations necessarily consist of densely packed RF elements; hence, a strong mutual coupling arise between them [11]. This issue is extremely significant both in the transmitting and receiving phase [15]. Indeed, the coupling worsen the coil reflection coefficient (due to the frequency splitting phenomenon), thus increasing the reflected energy amount and reducing the power efficiency. On the other hand, the mutual cross talking dramatically spoils the received signal, with consequently image degradation.

However, the unquestioned arrays' advantages have motivated a considerable effort in the literature to face and mitigate the mutual coupling issue. The first appeared solution consists in the partial overlap of strictly adjacent array coils [6]. This method can be straightforwardly applied but it produces inevitably a decrease in the useful FoV and it may be not always easily scalable when the number of RF coils increases, requiring additional means for decoupling. More recently, the Induced Current Elimination (ICE) technique has been introduced [15]–[17]; it exploits additional resonant elements to be inserted between the RF coils in order to obtain the decoupling conditions. Such conditions can be retrieved based on an eigenvectors and eigenvalues approach. Similar to the ICE method, also the Magnetic Walls have been presented [18], [19]. Differently from ICE, here a high number of square miniaturized resonators are employed instead of a single one. Besides, different works reported in the literature for decoupling purposes, exploit additional reactive and resonant elements, variously interleaved between the MRI RF array coils [20]–[26]. In particular, the capacitive decoupling has been proved efficient when geometrically complex array configurations are used [27]–[30].

In this paper, we introduce a novel analytical framework to analyze the complex interactions between all the elements of an MRI array and to design an opportune filter for their decoupling using passive counter-coupled resonators as unit-cells. A related approach was first presented in [31]–[33] for the simple case of two concentric RF loops in a Dual Tuned configuration (^{1}H/^{23}Na). Here, we generalize such approach, modeling and also considering the coupling between next-nearest neighbors coils pairs, as required for typical phased arrays. Thanks to the proposed analytical framework, a deep physical comprehension of the system under consideration can be achieved, facilitating the design process. Indeed, we can determine the minimum number of passive resonators and their required self-impedance to obtain the mutual coupling reduction between the array elements, simultaneously minimizing the undesired resistive losses. Further, the designed filter can be printed on the same dielectric substrate of the MRI RF coils, thus the fabrication process is easy and controllable. Moreover, since no physical connections are present, the system is mechanically robust.

The paper is organized as follows. In Section II the analytical framework to analyze an array and to design the decoupling filter is presented; next, Section III is devoted to evaluate the developed theory on an exemplificative test-case,
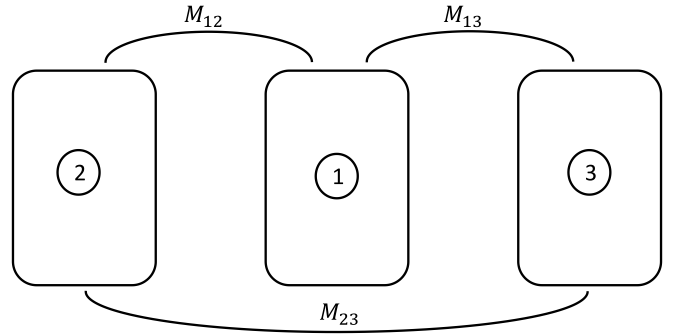

FIGURE 1. Schematic picture depicting the mutual interactions between three adjacent RF coils; the mutual coupling coefficients between strictly adjacent (M_{12} and M_{13}) and next-nearest neighbors (M_{23}) are highlighthed.

reporting the design, the full-wave simulations and the experimental results obtained over a fabricated prototype. Finally, Conclusions are presented in Section IV.

II. METHODS
As anticipated, the proposed decoupling method is based on an analytical framework that is useful to achieve a deep physical comprehension of the different mutual interactions between the elements of an MRI array. By considering both the mutual coupling coefficients between strictly adjacent and next-nearest neighbors coils (i.e., the most important coupling effects within an MRI array), the method can be used to describe arbitrary array configurations, provided to accurately take into account the specific geometrical arrangement. Moreover, the underlying circuital model provides quantitative and easy-to-handle parameters; through their manipulation, a full filter design can be achieved. As introduced before, the filter is based on the insertion of a limited number of passive resonators (such as spiral or split-ring resonators), carefully designed and placed between the array elements. The adopted assumptions and the corresponding analytical design framework are reported in the next paragraphs.

A. MAGNETO-STATIC COUPLING ESTIMATION
In order to realize a decoupling filter, the first step consists in the evaluation of the mutual interactions between all the array RF coils pairs; in particular, strictly adjacent coils and next-nearest neighbors pairs must be both considered (Fig. 1).

As already described in [33], under magneto-static hypothesis, we can apply the Biot-Savart formulation to estimate the mutual coupling between two generic RF coils [34], [35]. Indeed, the main contribution to mutual coupling at the MRI frequencies is the inductive one [36]. Hence, the magnetic field produced by a given current path in a specific point can be expressed as:

$$\vec{B}\left(\vec{r}\right) = \frac{\mu_0}{4\pi}\int \frac{I\,\vec{dl}\times\vec{r'}}{\left|\vec{r'}\right|^3} \tag{1}$$

where μ_0 (H/m) is the magnetic permeability of the vacuum, I (A) is the current amplitude flowing in the path, $\overrightarrow{dl}$ (m) is an infinitesimal element of the current path and $\overrightarrow{r'}$ (m) is the vector distance between the infinitesimal element $\overrightarrow{dl}$ and a generic point of the space.

The mutual coupling coefficient between coils i and j can be calculated as the magnetic flux per unit current through the surface of coil j induced by the current flowing in coil i:

$$M_{ij} = \frac{\Phi_{ij}}{I_i} \tag{2}$$

In this way, given the geometrical designs, we can numerically implement eqs. (1) and (2) to retrieve the mutual coupling coefficients between the considered RF coils.

Clearly, also the coupling between each RF coil and the filter unit-cell can be evaluated following the same formulation; hence, a proper filter able to compensate the undesired mutual coupling between the RF coils can be designed, as explained in the next section.

B. FILTER ANALYTICAL FORMULATION

Let suppose that N filtering unit-cells are inserted longitudinally in the space between each couple of adjacent MRI coils, as depicted in Fig. 2.

In particular, due to the small resonators footprint, it is possible to place the filtering unit-cells between two adjacent MRI coils sufficiently apart in order to assume the mutual coupling between them negligible (i.e., they are all independent each other). Moreover, due to symmetry reasons (Fig. 2), the same current is flowing in each unit-cell. Thus, from a circuital point of view, we can consider globally only a filtering element between two adjacent RF coils (respectively, numbered 4 and 5 in Fig. 2); obviously, the relative terms in the circuital equations have to be multiplied by the number of independent unit-cells N present between two adjacent RF coils [33].

Therefore, the entire system equations can be written as:

$$\begin{cases} Z_{11}I_1 + Z_{12}I_2 + Z_{13}I_3 + NZ_{14}I_4 + NZ_{15}I_5 = V_1 \\ Z_{21}I_1 + Z_{22}I_2 + Z_{23}I_3 + NZ_{24}I_4 + NZ_{25}I_5 = V_2 \\ Z_{31}I_1 + Z_{32}I_2 + Z_{33}I_3 + NZ_{34}I_4 + NZ_{35}I_5 = V_3 \\ NZ_{41}I_1 + NZ_{42}I_2 + NZ_{43}I_3 + NZ_{44}I_4 + NZ_{45}I_5 = 0 \\ NZ_{51}I_1 + NZ_{52}I_2 + NZ_{53}I_3 + NZ_{54}I_4 + NZ_{55}I_5 = 0 \end{cases} \tag{3}$$

Specifically, we indicate with I_4 the current flowing in each filtering unit-cell between RF coils 1 and 2; I_5 represents the same quantity but for the unit-cells between RF coils 1 and 3. I_1, I_2 and I_3 are the current flowing in the corresponding RF coils, whereas V_1, V_2 and V_3 describes their feeding RF generators.

At this point, we consider that the system depicted in Fig. 2 presents several other symmetries to be exploited; indeed, the filter unit-cells 4 and 5 interact equally with the RF coils. Hence:

$$\begin{cases} I_4 = I_5 \\ Z_{14} = Z_{41} = Z_{15} = Z_{51} \\ Z_{24} = Z_{42} = Z_{35} = Z_{53} \\ Z_{25} = Z_{52} = Z_{34} = Z_{43} \end{cases} \tag{4}$$
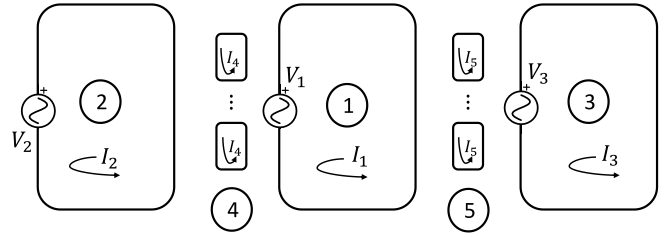

FIGURE 2. Schematic representation of the system under consideration: the three RF coils (numbered 1, 2 and 3) are interleaved with N filtering elements (globally numbered 4 and 5).

Thus, the system (3) can be simplified using (4) in the following manner.

$$\begin{cases} Z_{11}I_1 + Z_{12}I_2 + Z_{13}I_3 + 2NZ_{14}I_4 = V_1 \\ Z_{21}I_1 + Z_{22}I_2 + Z_{23}I_3 + N(Z_{24}+Z_{25})I_4 = V_2 \\ Z_{31}I_1 + Z_{32}I_2 + Z_{33}I_3 + N(Z_{34}+Z_{35})I_4 = V_3 \\ 2Z_{41}I_1 + (Z_{42}+Z_{52})I_2 + (Z_{43}+Z_{53})I_3 + \\ \quad + 2(Z_{44}+Z_{45})I_4 = 0 \end{cases} \tag{5}$$

In particular, we have condensed the two equations corresponding to the filter unit-cells 4 and 5 into a single condition (from now on, numbered 4), thanks to the previously observed symmetries. Then, we can express the current flowing in the filter unit-cells I_4 as a function of the RF coils currents (I_1, I_2 and I_3) and operate a substitution. Thus, the corresponding impedance matrix of the three RF coils in the presence of the decoupling SRs can be now derived.

$$\begin{pmatrix} Z_{11} - \frac{2NZ_{14}Z_{41}}{(Z_{44}+Z_{45})} & Z_{12} - \frac{NZ_{14}(Z_{24}+Z_{25})}{(Z_{44}+Z_{45})} & \cdots \\ Z_{21} - \frac{NZ_{41}(Z_{24}+Z_{25})}{(Z_{44}+Z_{45})} & Z_{22} - \frac{N(Z_{24}+Z_{25})^2}{2(Z_{44}+Z_{45})} & \cdots \\ Z_{31} - \frac{NZ_{41}(Z_{34}+Z_{35})}{(Z_{44}+Z_{45})} & Z_{32} - \frac{N(Z_{24}+Z_{25})(Z_{43}+Z_{53})}{2(Z_{44}+Z_{45})} & \cdots \\ Z_{13} - \frac{NZ_{14}(Z_{43}+Z_{53})}{(Z_{44}+Z_{45})} \\ Z_{23} - \frac{N(Z_{24}+Z_{25})(Z_{43}+Z_{53})}{2(Z_{44}+Z_{45})} \\ Z_{33} - \frac{N(Z_{34}+Z_{53})^2}{2(Z_{44}+Z_{45})} \end{pmatrix} \tag{6}$$

Specifically, in order to decouple the RF coils, it is ideally required that the following elements are nulled (and, thus, making the system impedance matrix diagonal).

$$\begin{cases} Z_{12} - \frac{NZ_{14}(Z_{24}+Z_{25})}{(Z_{44}+Z_{45})} = 0 \\ Z_{13} - \frac{NZ_{14}(Z_{43}+Z_{53})}{(Z_{44}+Z_{45})} = 0 \\ Z_{23} - \frac{N(Z_{24}+Z_{25})(Z_{43}+Z_{53})}{2(Z_{44}+Z_{45})} = 0 \end{cases} \tag{7}$$

Referring to the symmetries conditions described in (4), we can notice that the first two equations of the system (7) are equivalent. Hence, the decoupling conditions can be derived from the first and third equations of (7).

As already presented in [33] and as speculated in the previous Section II-A, we suppose that the mutual terms in (7) are all in the form $Z_{ij} = j\omega M_{ij}$ (i.e., inductive coupling). Instead, the Z_{ii} terms can be expressed as a classical RLC series self-impedance ($R_{ii}+j\omega L_{ii}+1/j\omega C_{ii}$). In that condition, each equation of (7) present a real and an imaginary term.

The imaginary terms can be perfectly nulled by applying the following conditions, analogously to what derived

in [33]:

$$\begin{cases} \frac{N M_{14}(M_{24}+M_{25})}{M_{12}} = X_{4_{tot}} \\ \frac{N(M_{24}+M_{25})^2}{2M_{23}} = X_{4_{tot}} \end{cases} \qquad (8)$$

where N is the number of filtering unit-cells interleaved between two adjacent RF coils and $X_{4_{tot}}$ is the unit-cell reactive self-impedance required for the coupling compensation at the desired working frequency:

$$X_{4_{tot}} = (L_4 + M_{45}) - \frac{1}{\omega^2 C_4} \qquad (9)$$

Hence, from (8), we can immediately evaluate the reactive self-impedance value that the single filter unit-cell must retain. Moreover, the mutual coupling terms of the system must satisfy another condition, that can be obtained by equating the left terms of both the expressions (8):

$$M_{14}(2M_{23} - M_{12}) - M_{12}M_{25} = 0 \qquad (10)$$

Thus, satisfying (8)-(10) will lead to the compensation of the imaginary terms of the mutual coupling between the MRI array elements.

At this point, we are interested in the minimization of the real term of the equations (7). In particular, as described in [33], the condition to maintain the real term negligible is the following:

$$\omega^2 X_{4_{tot}}^2 \gg R_4^2 \qquad (11)$$

where R_4 is the unit-cell self-resistance. Substituting $X_{4_{tot}}$ from the relations (8) in (11), these expressions on the minimum required number of filter unit-cells to minimize the real mutual coupling terms can be derived.

$$\begin{cases} N^2 \gg \left[\frac{M_{12}R_4}{\omega M_{14}(M_{24}+M_{25})}\right]^2 \\ N^2 \gg \left[\frac{2M_{23}R_4}{\omega(M_{24}+M_{25})^2}\right]^2 \end{cases} \qquad (12)$$

In summary, the satisfaction of (8), (10) and (12) guarantees the decoupling between the array elements, both for strictly adjacent and next-nearest pairs, with low level of losses. In the next section, we present an *ad-hoc* test-case to verify the model effectiveness in a practical situation.

III. TEST CASE
We herein describe the results obtained applying the proposed analytical method on a significant test-case. Indeed, we designed, simulated and fabricated a 3-element ^{1}H RF planar array for a 7 T MRI scanner with a suitable decoupling filter realized with spiral resonators.

A. ANALYTICAL DESIGN OF THE FILTER
The adopted array consisted of 3 identical rectangular RF loops with external size of 13 cm × 6 cm, whereas the gap between them is 2.8 cm (Fig. 3).

Considering the chosen array geometry, we decided to realize the unit-cell of the filter by using two closely placed SRs. In this way, we guaranteed a sufficient value of mutual
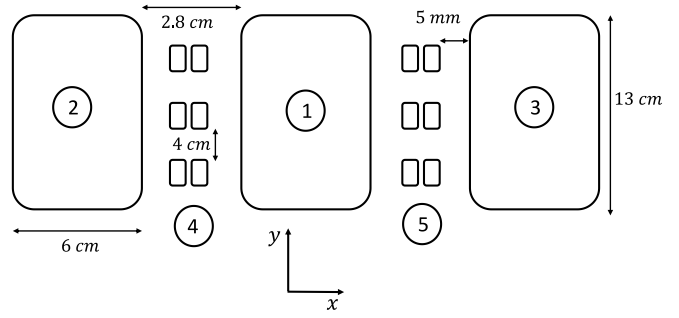

FIGURE 3. 3-element array chosen as test-case: the size of the coils and their gaps are reported for clarity. In addition, the filter's unit-cells are also included in the picture (drawings not in scale).

coupling between the single filter's unit-cell and the RF coils, necessary for obtaining a satisfactory interaction (and decoupling) level. In this case, the two SRs constituting the unit-cell are strongly coupled, thus we have to consider this aspect. Specifically, for symmetry reasons, they interact equally with the surrounding RF array coils and, thus, the currents flowing in each of them are the same; hence, it is sufficient to consider only one equation to describe both of them from a circuital point of view. Moreover, since their circulating current is equal, the total mutual coupling between this unit-cell and one of the RF coils is given by the sum of the single mutual coupling coefficients between each unit-cell's SR and the considered RF coil. Hence, the analytical model presented before is perfectly valid also in this condition by adopting such observations. Obviously, if the symmetrical disposition is not satisfied, these hypotheses cannot be applied, and it is required to add an extra element to the model.

At first glance, the derived decoupling conditions (8), (10) and (12) may appear not easy to be applied and fulfilled for the filter design. However, in several practical situations, important simplifications can be adopted. For instance, referring to Fig. 3, the mutual coupling M_{25} between the RF coil 2 and the filtering unit-cells 5 (and, analogously, between coil 3 and the filtering unit-cells 4, M_{34}) can be very often neglected. Indeed, spiral resonators are very miniaturized inclusions whose electromagnetic field is strictly confined in the very nearby of their structure. For the same reason, the mutual coupling M_{45} between the filtering unit-cells 4 and 5 can be generally omitted.

With these observations in mind, as indicated in Section II, we first estimated the mutual coupling existing between strictly adjacent and next-neighbors RF coils pairs (i.e., M_{12} and M_{23} referring to eq. (8) and Fig. 3) through the magnetostatic approach. The strictly adjacent coils presented a mutual coupling value of −12.5 nH, whereas M_{23} was equal to −6.6 nH.

Considering the geometry and the available space, we inserted 3 unit-cells between each strictly adjacent RF coils pair (Fig. 3). For the design of the single SR and their exact positioning, we exploited the spiral design procedure
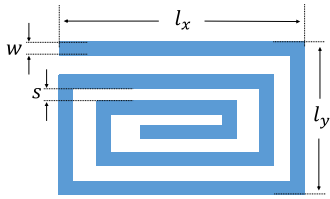
FIGURE 4. Pictorial representation of the adopted miniaturized spiral resonator (draw not in scale).

explained in details in [33], [37]. We realized a rectangular, 6 turns SR, with external dimensions of 13.7 mm × 6.7 mm, strip width w 0.127 mm and gap s between two adjacent branches equal to 0.127 mm (Fig. 4). As said before, the filter's unit-cell consisted of two adjacent SRs, aligned along their major axis and separated by 4.6 mm (see Fig. 3 for a graphical representation). In this way, the unit-cell extremities are 5 mm away, along the x-axis, from the nearby RF coils (we took care to maintain the geometrical symmetry). Following the SRs characterization method described in [35], and taking into account that this spiral is placed close to another one (whose mutual coupling have to be considered), it presented an overall inductance of 737 nH and a self-capacitance of 0.375 pF (L_4 and C_4 in (9)). Each unit-cell is positioned 4 cm away from the neighbor one, along the y-axis (Fig. 3), guaranteeing that the mutual coupling between them is negligible (as required from the theoretical model). Employing the Biot-Savart formulation, we estimated the mutual coupling between the individual unit-cell and the RF coils close to it (i.e., M_{14} and M_{24} in eq. (8)). As explained, for the chosen symmetrical disposition, it consists in the sum of the mutual coupling coefficients between the considered RF coil and the two SRs of the unit-cell; it globally resulted in 9.8 nH. Conversely, the mutual coupling between two adjacent unit-cells (separated by 4 cm along the y-axis) was around 0.4 nH (thus negligible, as required).

As observed, some other terms can be simplified studying the geometry of the system. In particular, the M_{25} term resulted in a value of 0.25 nH, thus not significant with respect to M_{24} in eq.(8). Finally, the term M_{45} (i.e., the mutual coupling between the opposed filter's elements within the array) is also very small (~0.1 nH), thus it can be discarded with respect to L_4 in eq. (9).

Substituting the estimated values in one of the eq. (8), we obtained for the required reactive impedance of the unit-cell (i.e., $X_{4_{tot}}$) the value of −23.05 nH. Using (9), we evaluated the actual reactive self-impedance of the chosen unit-cell at the desired working frequency (at 298 MHz): it resulted in −24.4 nH, hence able to compensate the undesired mutual coupling.

Under the hypothesis that M_{25} is negligible (as effectively proved), the condition (10) simply becomes $M_{12} = 2M_{23}$, in good agreement with the estimation of the mutual coupling between strictly adjacent and next-neighbors RF coils pairs above mentioned ($M_{12} = -12.5$ vs $M_{23} = -6.6$ nH).
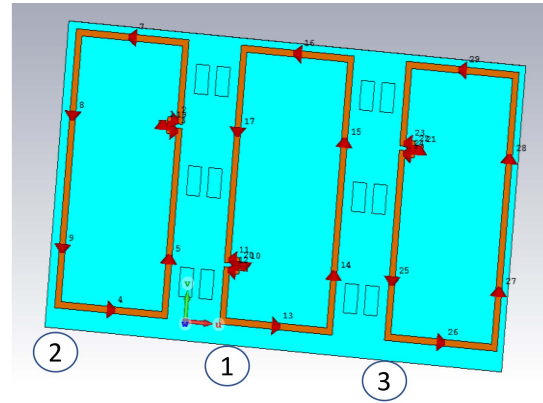
(a)
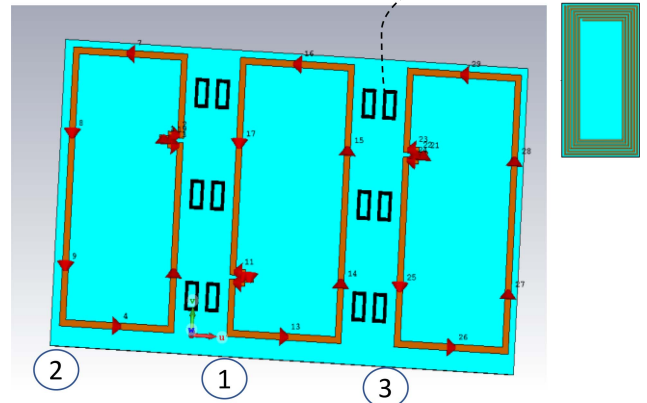
(b)

FIGURE 5. CST CAD models of the adopted RF array without (a) and with (b) filtering spiral resonators. An inset of the single resctangular, 6-turn spiral resonator is shown for more clarity.
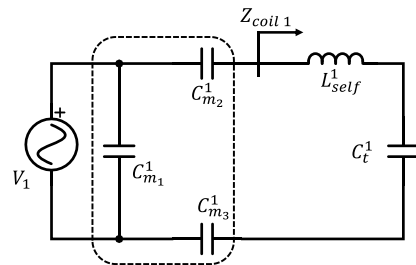

FIGURE 6. Adopted capacitive matching network. The superscripted index is referred to the RF coil number, as reported in Fig. 5.

Eventually, it would be possible to better match this condition by opportunely changing the relative position of the RF coils.

As the last step, we verified the conditions reported in (12) about the minimization of the real term of the mutual coupling. For $N=3$ (i.e., the number of unit-cells interposed between strictly adjacent MRI loops), we obtained $9 \gg 0.48$ for the first condition and $9 \gg 0.75$ for the second one; hence, the filter design simultaneously satisfied the conditions (8), (10) and (12) required for an effective decoupling
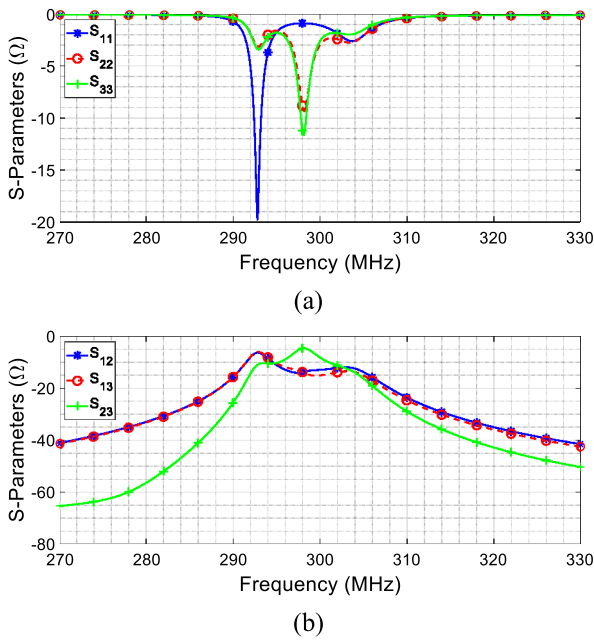
(a)

(b)

FIGURE 7. Simulated S-parameters of the 3 array elements before the filter insertion. (a) S_{11}, S_{22}, S_{33}; (b) S_{12}, S_{13}, S_{23}. It can be highlighted the significant coupling level between the three elements.
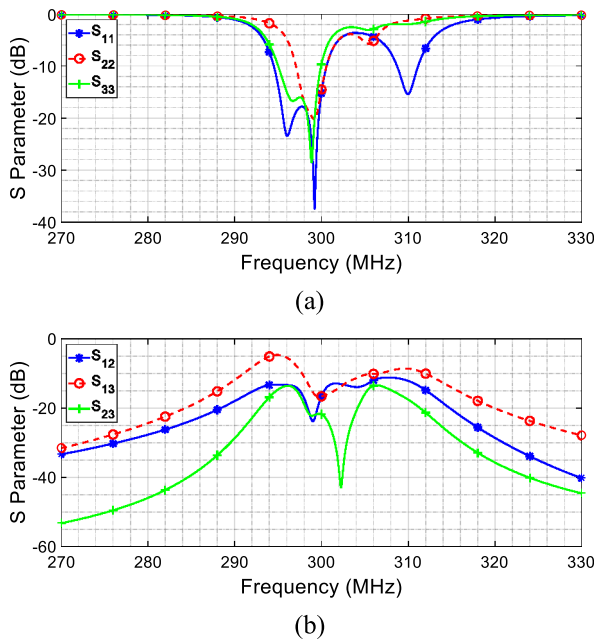

(a)

(b)

FIGURE 8. Simulated S-parameters of the 3 array elements after the filter insertion. (a) S_{11}, S_{22}, S_{33}; (b) S_{12}, S_{13}, S_{23}. The presence of the designed filter produces a significant decoupling level, while preserving good matching and tuning levels.

(a)

(b)

FIGURE 9. Fabricated PCB array prototype without decoupling filter (a). Fabricated PCB array prototype with the filter: the inset shows the spiral resonator geometry in details (b).
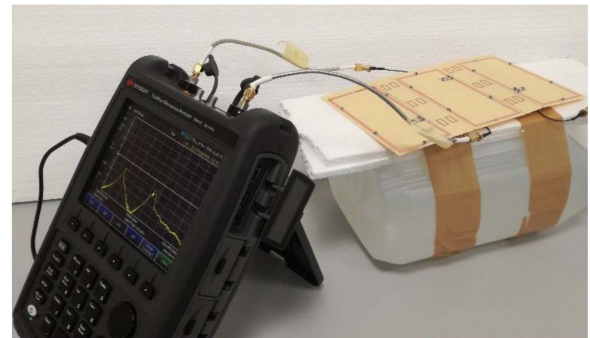

FIGURE 10. Photo showing the employed VNA and the RF array in the presence of a saline biological phantom.

a proper verification and validation, significant simplification can be adopted, making easier and effective the overall design process. As demonstrated in [33], it may be also worth highlighting that similar analytical approaches are sufficiently robust with respect to various error sources (for instance, the adopted magneto-static approximation and the spiral resonator e.m. characterization) and can be applied with confidence.

B. FULL-WAVE SIMULATIONS
After the analytical design part, we performed full-wave simulations (CST Studio Suite, Darmstadt) in order to verify the developed solution before fabricating prototypes. Hence, we realized the CAD model following the geometrical constraints described in the previous section. In particular, for the RF coils, we used a 3.2 mm width copper strip, etched on a 0.8 mm thick dielectric substrate (Arlon, ε_r=3.45, tanδ=0.0035) (Fig. 5(a)). On the same dielectric substrate, we also printed the decoupling spiral resonators (Fig. 5(b)).

of the RF array elements at the desired working frequency (298 MHz).

In summary, the circuital model herein presented is general and considers all the possible interactions between the different components of a common planar RF MRI array in presence of SRs as decoupling unit-cells. However, after
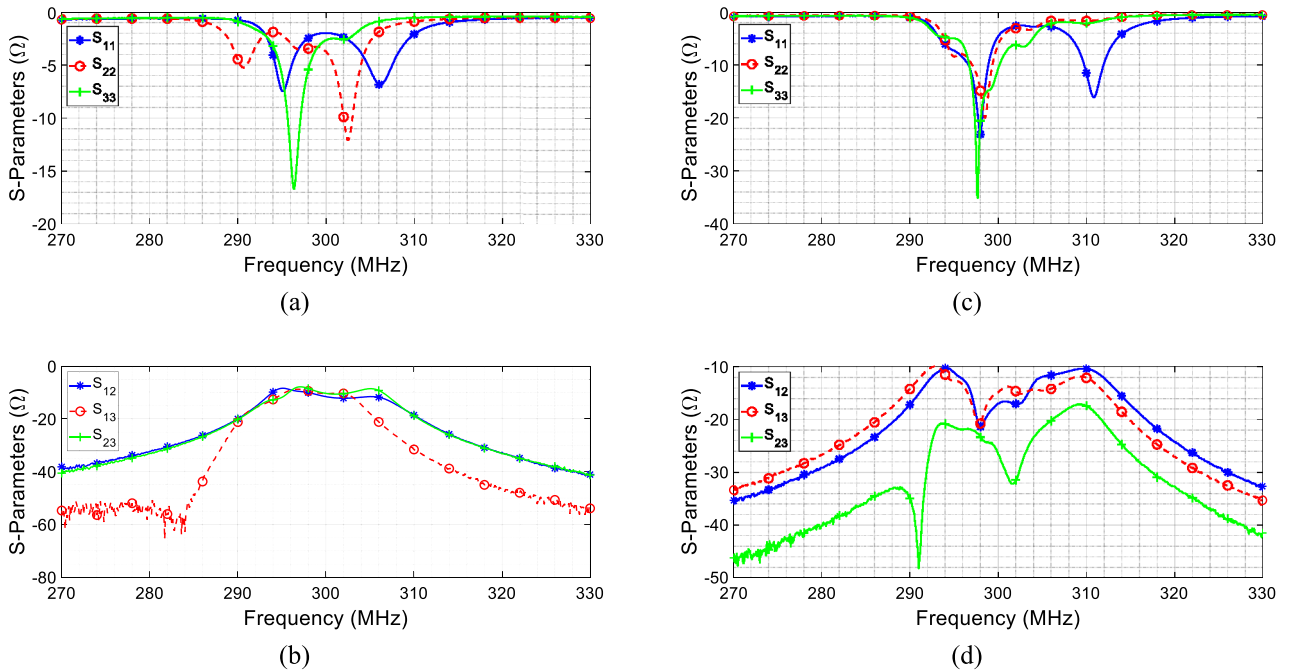
FIGURE 11. Measured S-parameters without (left column) and with (rigth column) the decoupling SRs filter, in the absence of a biological phantom. It can be noticed the high mutual coupling levels between the MRI coils when no filter is adopted and the consequential RF coils detuning (a)–(b). Instead, the designed filter is able to restore a good tuning and matching level at the desired working frequency (298 MHz) together with an excellent decoupling level (better than −20 dB) (c)-(d).

TABLE 1. Matching and tuning capacitors of the ^{1}H RF coils without filter.

Capacitors	Function	Value
$C_{t_1}^1, C_{t_2}^1, C_{t_3}^1, C_{t_4}^1, C_{t_5}^1$	Tuning coil 1	9 pF
$C_{t_1}^2, C_{t_2}^2, C_{t_3}^2, C_{t_4}^2, C_{t_5}^2$	Tuning coil 2	9 pF
$C_{t_1}^3, C_{t_2}^3, C_{t_3}^3, C_{t_4}^3, C_{t_5}^3$	Tuning coil 3	9 pF
$C_{m_1}^1, C_{m_1}^2, C_{m_1}^3$	Matching	26.1 pF
$C_{m_2}^1, C_{m_2}^2, C_{m_3}^3, C_{m_3}^1, C_{m_3}^2, C_{m_3}^3$	Matching	3.1 pF

TABLE 2. Matching and tuning capacitors of the ^{1}H RF coils with filter.

Capacitors	Function	Value
$C_{t_1}^1, C_{t_2}^1, C_{t_3}^1, C_{t_4}^1, C_{t_5}^1$	Tuning coil 1	8 pF
$C_{t_1}^2, C_{t_2}^2, C_{t_3}^2, C_{t_4}^2, C_{t_5}^2$	Tuning coil 2	8 pF
$C_{t_1}^3, C_{t_2}^3, C_{t_3}^3, C_{t_4}^3, C_{t_5}^3$	Tuning coil 3	8 pF
$C_{m_1}^1$	Matching	9 pF
$C_{m_1}^2, C_{m_1}^3$	Matching	13.7 pF
$C_{m_2}^1, C_{m_3}^1$	Matching	4.1 pF
$C_{m_2}^2, C_{m_3}^2, C_{m_2}^3, C_{m_3}^3$	Matching	4.5 pF

Firstly, the single ^{1}H RF coil was tuned and 50 Ω-matched at 298 MHz using opportune capacitors. Specifically, we equally distributed 5 series tuning capacitor (C_t) along the loop and we designed a balanced capacitive matching network (see Table 1 for the lumped elements values and Fig. 6 for the adopted matching network configuration). After that, we placed together the three RF coils, in a coplanar fashion and separated by 2.8 cm, as depicted in Fig. 5(a). The obtained S-parameters are reported in Fig. 7; it can be noticed a significant detuning of the coils and high coupling levels (up to −4.7 dB) that make such configuration not able to perform imaging correctly.

The next step consisted in the insertion of the designed filter (Fig. 5(b)). Naturally, we had to change the tuning and matching capacitors values, as reported in Table 2. Fig. 8 shows the obtained S-parameters; beside a good tuning and matching level for the three RF coils, it is worth pointing out also the excellent decoupling levels (better than −17 dB) at the desired working frequency (298 MHz).

In summary, the full-wave simulations demonstrated the validity of the developed analytical framework. However, since we are working with small and nested resonators, one possible concern can be the actual power handling limits of these structures during a high power stimulus. Nonetheless, this decoupling solution adopting SRs has been proved in [33] to have good power handling properties (up to 4 kWpp), thus demonstrating its practical feasibility.

C. EXPERIMENTAL VERIFICATION
Finally, we fabricated a prototype of the array under analysis, using PCB technology. The RF coils and the filtering SRs were printed adopting the geometrical specifications and materials prescribed in the previous section, using a 35 μm thick etched copper strip. We soldered appropriate SMD capacitors to the RF coils, following the values reported in Tables 1 and 2; in particular, we substituted one tuning and
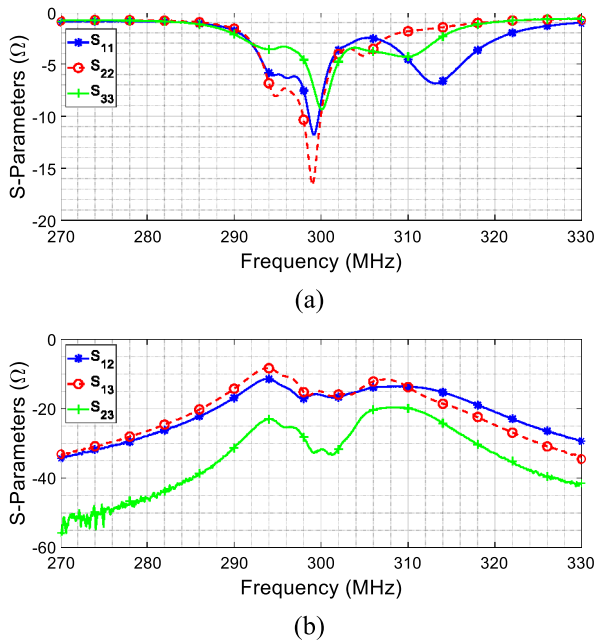
FIGURE 12. Measured S-parameters with the decoupling filter and in presence of a close biological phantom. It can be highlighted the good decoupling performance even with a very close biological load (decoupling always better than −16 dB).

one matching capacitor for each coil with variable ones, in order to limit the effects of tolerances and fabrication imperfections. Fig. 9 shows the realized prototypes with and without the decoupling filter.

Then, we measured at the VNA (N9918A, FieldFox Series, Keysight) the S-parameters for the two configurations (with and without filter), and in two different loading conditions. Indeed, the first round of measurements was acquired without any biological load; after that, we exposed the array to a saline solution phantom (ε_r=59, σ=0.58 S/m), placed 2 cm away from the MRI coils though an opportune spacer (Fig. 10). Fig. 11 and Fig. 12 summarizes the obtained results. It is worth highlighting that the measurements confirmed the validity of the analytical approach herein presented, being in good agreement with simulations. In particular, the decoupling level at the desired working frequency (298 MHz) is better than −21 dB without the phantom and better than −16 dB with the close presence of the saline solution. In addition, the tuning and matching levels are satisfying in both the cases.

Finally, as demonstrated in the literature [33], it may be also important to notice that the typical losses of the filtering SRs are quite low and aligned with other decoupling techniques, thus not representing a particular concern.

IV. CONCLUSION
In this paper, we presented an analytical circuital framework to design decoupling filters for RF MRI array elements exploiting counter-coupled passive resonators as unit-cells.

By using a test-case – a 3-element ^{1}H RF array for 7T scanners –, we demonstrated the validity of the developed design method through full-wave simulations, obtaining an excellent agreement between theoretical and numerical results. After that, we fabricated a PCB prototype of the entire system, evaluating the actual filter decoupling performance in air and in the presence of a saline biological phantom. In every case, we achieved good decoupling levels both between strictly adjacent and next-nearest neighbors RF coils pairs, proving the feasibility and the effectiveness of the technique.

In particular, the proposed circuital model allows a deep comprehension of the different interactions between the system's components, aiding the designer to realize a good decoupling solution from scratch thanks to quantitative and simple-to-manipulate parameters. Then, only few and targeted full-wave simulations can be carried out to refine the filter design before realizing the actual prototype. Moreover, the possibility to print both the RF coils and the decoupling resonators on the same dielectric substrate leads to a mechanically robust experimental set-up. Hence, this work can pave the way to an easy and effective use of passive resonators to obtain satisfying decoupling levels for RF MRI array elements with a robust and repeatable fabrication process. Future developments can be directed to perfectionate the model, further improving the decoupling performance.

REFERENCES
[1] J. T. Vaughan *et al.*, "7T vs. 4T: RF power, homogeneity, and signal-to-noise comparison in head images," *Magn. Reson. Med.*, vol. 46, no. 1, pp. 24–30, 2001.

[2] G. Adriany *et al.*, "Transmit and receive transmission line arrays for 7 Tesla parallel imaging," *Magn. Reson. Med.*, vol. 53, no. 2, pp. 434–445, 2005.

[3] X. Zhang, K. Ugurbil, R. Sainati, and W. Chen, "An inverted-microstrip resonator for human head proton MR imaging at 7 tesla," *IEEE Trans. Biomed. Eng.*, vol. 52, no. 3, pp. 495–504, Mar. 2005.

[4] C. M. Collins *et al.*, "Different excitation and reception distributions with a single-loop transmit-receive surface coil near a head-sized spherical phantom at 300 MHz," *Magn. Reson. Med.*, vol. 47, no. 5, pp. 1026–1028, 2002.

[5] T. S. Ibrahim, R. Lee, B. A. Baertlein, A. M. Abduljalil, H. Zhu, and P.-M. L. Robitaille, "Effect of RF coil excitation on field inhomogeneity at ultra high fields: A field optimized TEM resonator," *Magn. Reson. Imag.*, vol. 19, no. 10, pp. 1339–1347, 2001.

[6] P. B. Roemer, W. A. Edelstein, C. E. Hayes, S. P. Souza, and O. M. Mueller, "The NMR phased array," *Magn. Reson. Med.*, vol. 16, no. 2, pp. 192–225, 1990, doi: 10.1002/mrm.1910160203.

[7] D. K. Sodickson and W. J. Manning, "Simultaneous acquisition of spatial harmonics (SMASH): Fast imaging with radiofrequency coil arrays," *Magn. Reson. Med.*, vol. 38, no. 4, pp. 591–603, 1997.

[8] K. P. Pruessmann, M. Weiger, M. B. Scheidegger, and P. Boesiger, "SENSE: Sensitivity encoding for fast MRI," *Magn. Reson. Med.*, vol. 42, no. 5, pp. 952–962, 1999.

[9] M. Weiger, K. P. Pruessmann, and P. Boesiger, "Cardiac real-time imaging using SENSE," *Magn. Reson. Med.*, vol. 43, no. 2, pp. 177–184, 2000.

[10] J. A. de Zwart, P. J. Ledden, P. van Gelderen, J. Bodurka, R. Chu, and J. H. Duyn, "Signal-to-noise ratio and parallel imaging performance of a 16-channel receive-only brain coil array at 3.0 Tesla," *Magn. Reson. Med.*, vol. 51, no. 1, pp. 22–26, 2004, doi: 10.1002/mrm.10678.

[11] G. Adriany *et al.*, "A 32-channel lattice transmission line array for parallel transmit and receive MRI at 7 tesla," *Magn. Reson. Med.*, vol. 63, no. 6, pp. 1478–1485, 2010.

[12] B. Keil and L. L. Wald, "Massively parallel MRI detector arrays," *J. Magn. Reson.*, vol. 229, pp. 75–89, Apr. 2013.

[13] Y. Zhu, "Parallel excitation with an array of transmit coils," *Magn. Reson. Med.*, vol. 51, no. 4, pp. 775–784, 2004.

[14] B. Guérin, M. Gebhardt, S. Cauley, E. Adalsteinsson, and L. L. Wald, "Local specific absorption rate (SAR), global SAR, transmitter power, and excitation accuracy trade-offs in low flip-angle parallel transmit pulse design," *Magn. Reson. Med.*, vol. 71, no. 4, pp. 1446–1457, 2014.

[15] X. Yan, J. C. Gore, and W. A. Grissom, "New resonator geometries for ICE decoupling of loop arrays," *J. Magn. Reson.*, vol. 277, pp. 59–67, Apr. 2017, doi: 10.1016/j.jmr.2017.02.011.

[16] Y. Li, Z. Xie, Y. Pang, D. Vigneron, and X. Zhang, "ICE decoupling technique for RF coil array designs," *Med. Phys.*, vol. 38, no. 7, pp. 4086–4093, 2011, doi: 10.1118/1.3598112.

[17] X. Yan, X. Zhang, B. Feng, C. Ma, L. Wei, and R. Xue, "7T transmit/receive arrays using ICE decoupling for human head MR imaging," *IEEE Trans. Med. Imag.*, vol. 33, no. 9, pp. 1781–1787, Sep. 2014, doi: 10.1109/TMI.2014.2313879.

[18] X. Yan, X. Zhang, L. Wei, and R. Xue, "Magnetic wall decoupling method for monopole coil array in ultrahigh field MRI: A feasibility test," *Quant. Imag. Med. Surg.*, vol. 4, no. 2, p. 79, 2014.

[19] I. R. Connell, K. M. Gilbert, M. A. Abou-Khousa, and R. S. Menon, "Design of a parallel transmit head coil at 7T with magnetic wall distributed filters," *IEEE Trans. Med. Imag.*, vol. 34, no. 4, pp. 836–845, 2014.

[20] E. Georget *et al.*, "Stacked magnetic resonators for MRI RF coils decoupling," *J. Magn. Reson.*, vol. 275, pp. 11–18, Feb. 2017, doi: 10.1016/j.jmr.2016.11.012.

[21] N. I. Avdievich, J. W. Pan, and H. P. Hetherington, "Resonant inductive decoupling (RID) for transceiver arrays to compensate for both reactive and resistive components of the mutual impedance," *NMR Biomed.*, vol. 26, no. 11, pp. 1547–1554, 2013.

[22] B. Wu, P. Qu, C. Wang, J. Yuan, and G. X. Shen, "Interconnecting L/C components for decoupling and its application to low-field open MRI array," *Concepts Magn. Reson. B, Magn. Reson. Eng. Educ. J.*, vol. 31, no. 2, pp. 116–126, 2007.

[23] C. Von Morze *et al.*, "An eight-channel, nonoverlapping phased array coil with capacitive decoupling for parallel MRI at 3 T," *Concepts Magn. Reson. B, Magn. Reson. Eng. Educ. J.*, vol. 31B, no. 1, pp. 37–43, 2007.

[24] X. Zhang and A. Webb, "Design of a capacitively decoupled transmit/receive NMR phased array for high field microscopy at 14.1 T," *J. Magn. Reson.*, vol. 170, no. 1, pp. 149–155, 2004.

[25] X. Yan, J. C. Gore, and W. A. Grissom, "Self-decoupled radiofrequency coils for magnetic resonance imaging," *Nat. Commun.*, vol. 9, no. 1, p. 3481, Dec. 2018, doi: 10.1038/s41467-018-05585-8.

[26] B. Wu, X. Zhang, P. Qu, and G. X. Shen, "Design of an inductively decoupled microstrip array at 9.4 T," *J. Magn. Reson.*, vol. 182, no. 1, pp. 126–132, 2006.

[27] I. A. Elabyad, M. Terekhov, M. R. Stefanescu, D. Lohr, M. Fischer, and L. M. Schreiber, "Design and evaluation of a novel symmetric multichannel transmit/receive coil array for cardiac MRI in pigs at 7 T," *IEEE Trans. Microw. Theory Techn.*, vol. 67, no. 9, pp. 3928–3945, Sep. 2019, doi: 10.1109/TMTT.2019.2913636.

[28] I. A. Elabyad, M. Terekhov, M. R. Stefanescu, D. Lohr, M. Fischer, and L. M. Schreiber, "Design of a novel antisymmetric coil array for parallel transmit cardiac MRI in pigs at 7 T," *J. Magn. Reson.*, vol. 305, pp. 195–208, Aug. 2019, doi: 10.1016/j.jmr.2019.07.004.

[29] A.-L. Perrier *et al.*, "Design of a two-channel NMR coil using an impedance transformation approach," *IEEE Sens. J.*, vol. 12, no. 6, pp. 1801–1808, Jun. 2012, doi: 10.1109/JSEN.2011.2178237.

[30] A. Gräßl *et al.*, "Design, evaluation and application of an eight channel transmit/receive coil array for cardiac MRI at 7.0T," *Eur. J. Radiol.*, vol. 82, no. 5, pp. 752–759, May 2013, doi: 10.1016/j.ejrad.2011.08.002.

[31] D. Brizi, N. Fontana, F. Costa, G. Tiberi, and A. Monorchio, "On the optimization of distributed magnetic traps in MRI coils decoupling," in *Proc. IEEE Int. Symp. Antennas Propag. USNC/URSI Nat. Radio Sci. Meeting*, Jul. 2018, pp. 893–894, doi: 10.1109/APUSNCURSINRSM.2018.8608439.

[32] N. Fontana, D. Brizi, F. Costa, G. Tiberi, and A. Monorchio, "On the decoupling robustness of distributed magnetic traps in biological loaded dual tuned MR coils," in *Proc. IEEE Int. Symp. Antennas Propag. USNC-URSI Radio Sci. Meeting*, Jul. 2019, pp. 759–760, doi: 10.1109/APUSNCURSINRSM.2019.8889180.

[33] D. Brizi *et al.*, "Design of distributed spiral resonators for the decoupling of MRI double-tuned RF coils," *IEEE Trans. Biomed. Eng.*, vol. 67, no. 10, pp. 2806–2816, Oct. 2020, doi: 10.1109/TBME.2020.2971843.

[34] Y. Cheng and Y. Shu, "A new analytical calculation of the mutual inductance of the coaxial spiral rectangular coils," *IEEE Trans. Magn.*, vol. 50, no. 4, pp. 1–6, Apr. 2014.

[35] D. Brizi, N. Fontana, F. Costa, and A. Monorchio, "Accurate extraction of equivalent circuit parameters of spiral resonators for the design of metamaterials," *IEEE Trans. Microw. Theory Techn.*, vol. 67, no. 2, pp. 626–633, Feb. 2019, doi: 10.1109/TMTT.2018.2883036.

[36] A. M. Maunder, M. Daneshmand, P. Mousavi, B. G. Fallone, and N. De Zanche, "Stray capacitance between magnetic resonance imaging coil elements: Models and application to array decoupling," *IEEE Trans. Microw. Theory Techn.*, vol. 61, no. 12, pp. 4667–4677, Dec. 2013.

[37] F. Bilotti, A. Toscano, L. Vegni, K. Aydin, K. B. Alici, and E. Ozbay, "Equivalent-circuit models for the design of metamaterials based on artificial magnetic inclusions," *IEEE Trans. Microw. Theory Techn.*, vol. 55, no. 12, pp. 2865–2873, Dec. 2007.

DANILO BRIZI (Member, IEEE) born in Viterbo, Italy, 1992. He received the M.S. Laurea degree (*summa cum laude*) in biomedical engineering, and the Ph.D. degree in information engineering from the University of Pisa in 2016 and 2020, respectively, where he is currently working as a Postdoctoral Researcher. His research interests include hyperthermia with magnetic nanoparticles, MRI filter design, and wireless Power transfer applications.

NUNZIA FONTANA was born in Agrigento, Italy, in 1984. She received the M.Sc. degree (*summa cum laude*) in telecommunications engineering and the Ph.D. degree in remote sensing from the University of Pisa, Italy, in 2008 and in 2012, respectively. From 2012 to 2016, she was a Postdoctoral Researcher with the University of Pisa. From 2016 to 2019, she was a Researcher with the National Inter-University Consortium for Telecommunications. She is currently an Assistant Professor with the Department of Energy, Systems, Territory and Construction Engineering, University of Pisa. Her research activities have been published in several international scientific journals and in a number of international conference proceedings. Her research interests include: wireless power transfer; antennas, impedance matching networks design, prototyping, and RF testing; radio frequency coils design for magnetic resonance and RF testing and bio-electromagnetics. She is a member of ACES. He serves as an Associate Editor for *Applied Computational Electromagnetics Society Journal*.

AGOSTINO MONORCHIO (Fellow, IEEE) is a Full Professor with the University of Pisa. He spent several research periods with the Electromagnetic Communication Laboratory, Pennsylvania State University, USA. He has carried out considerable research activity and technical consultancy in national, EU, and U.S. industries, coordinating, as a principal scientific investigator, a large number of national and European research projects. The activity is mainly carried out with the Microwave and Radiation Laboratory, Department of Information Engineering, University of Pisa, together with a large group of Ph.D. students, postdoctoral fellows, and research associates. He is a member of the RaSS National Laboratory, Consorzio Nazionale Interuniversitario per le Telecomunicazioni. He is affiliated with the Pisa Section of INFN, the National Institute of Nuclear Physics in 2010. His research results have been published in more than 130 journal papers and book chapters, and more than 200 communications at international and national conferences. He has coauthored of four patents. He is active in a number of areas, including computational electromagnetics, microwave metamaterials, radio propagation for wireless systems, the design and miniaturization of antennas and electromagnetic compatibility, and biomedical microwaves applications.

Prof. Monorchio was a recipient of the Scholarship (Fellowship Award) of the Summa Foundation, New Mexico, USA, and the Framework of CNR-NATO Senior Fellowship Programme. He serves as reviewer for international journals. He was an Associate Editor of IEEE ANTENNAS AND WIRELESS PROPAGATION LETTERS from 2002 to 2007. He was an AdCom member from 2017 to 2019. He is a Co-Chair of the Industrial Initiative Committee of the IEEE APS. In 2012, he was elevated to Fellow grade by the IEEE for his contributions to computational electromagnetics and for application of frequency selective surfaces in metamaterials.